Mn-Doping Level Dependence on the Magnetic Response of $Mn_xFe_{3-x}O_4$ Ferrite Nanoparticles

Xabier Lasheras[a], Maite Insausti [a,b*], Jesús Martínez de la Fuente[c], Izaskun Gil de Muro [a,b], Idoia Castellanos-Rubio[b], Lourdes Marcano[d,e], Maria Luisa Fernández-Gubieda [a,d], A. Serrano[f,g], Rosa Martín-Rodriguez[h,i], Eneko Garaio[j], Jose Angel García[d], Luis Lezama [b]

[a.] BCMaterials, Basque Center for Materials, Applications and Nanostructures, UPV/EHU Science Park, E-48940 Leioa, Spain
[b.] Dpto. de Química Inorgánica, Universidad del País Vasco, UPV/EHU, E-48940 Leioa, Spain
[c.] Instituto de Ciencia de Materiales de Aragón, CSIC/Universidad de Zaragoza, c/Pedro Cebruna 12, 50009 Zaragoza, Spain
[d] Dpto. Electricidad y Electrónica, Universidad del País Vasco - UPV/EHU, 48940 Leioa, Spain
[e.] Helmholtz-Zentrum Berlin für Materialien und Energie, Albert-Einstein-Str. 15, 12489 Berlin, Germany.
[f.] SpLine, Spanish CRG BM25 Beamline, ESRF, 38000, Grenoble, France.
[g] Instituto de Ciencia de Materiales de Madrid, CSIC, Cantoblanco, 28049, Madrid, Spain.
[h] QUIPRE Department, University of Cantabria, Avda. de Los Castros 46, 39005 Santander, Spain.
[i] Dpto de Física, Universidad Pública de Navarra, Campus Arrosadia, Pamplona 31006, Spain.
[j] Dpto. de Física Aplicada II, Universidad del País Vasco - UPV/EHU, Leioa 48940, Spain.

Table S1. Amounts of used reagents, iron(III) acetylacetonate ($Fe(acac)_3$), manganese(II) acetylacetonate ($Mn(acac)_2$), oleic acid, oleylamine and 1,2-hexadecanediol, benzyl solvent volume and Fe:Mn metal rate in each synthesis.

Table S2. Nèel (τ_N), Brown (τ_B) and effective (τ_{eff}) relaxation times at room temperature calculated for all prepared samples. NP shape has been taken as spherical for all samples to perform this estimation.

Fig. S1. (A) X Ray diffraction patterns for ferrite nanoparticles. (B) (311) peak fitting for $Mn_{0.13}Fe_{2.87}O_4$ and $Mn_{0.13}Fe_{2.87}O_4$_G samples.

Fig. S2. Dynamic diameters of $Mn_{0.13}Fe_{2.87}O_4$, $Mn_{0.18}Fe_{2.82}O_4$, $Mn_{0.27}Fe_{2.73}O_4$, $Mn_{0.36}Fe_{2.64}O_4$ and $Mn_{0.13}Fe_{2.87}O_4$_G nanoparticle samples measured by DLS in 0.05 mgFe/mL toluene dispersions and expressed in % of total.

Fig. S3. Thermogravimetric curves for all prepared Mn ferrite nanoparticles measured in Ar atmosphere.

Fig. S4. M (H) cycles for all prepared Mn ferrite nanoparticles measured at 300 K in the VSM magnetometer in powder. The matrix effect in the final magnetization value has been discarded by diminishing the mass corresponding to organic matter.

Model S1. Modelling single magnetic domain with thermal fluctuations. Fokker-Planck equation.

Table S1. Amounts of used reagents, iron(III) acetylacetonate ($Fe(acac)_3$), manganese(II) acetylacetonate ($Mn(acac)_2$), oleic acid, oleylamine and 1,2-hexadecanediol, benzyl solvent volume and Fe:Mn metal rate in each synthesis.

	n (mmol)					V (mL)	
SAMPLE	**$Fe(acac)_3$**	**$Mn(acac)_2$**	**Oleic acid**	**Oleylamine**	**1,2-Hexadecanediol**	**Benzyl ether**	**Fe:Mn**
$Mn_{0.13}Fe_{2.87}O_4$	1.97	0.22	4.37	4.37	8.75	25	0.90:0.10
$Mn_{0.18}Fe_{2.82}O_4$	1.88	0.31	4.37	4.37	8.75	25	0.86:0.14
$Mn_{0.27}Fe_{2.73}O_4$	1.79	0.39	4.37	4.37	8.75	25	0.82:0.18
$Mn_{0.36}Fe_{2.64}O_4$	1.53	0.66	4.37	4.37	8.75	25	0.70:0.30
$Mn_{0.13}Fe_{2.87}O_4$_G	11.51	1.28	14.16	14.16	18.00	55	0.90:0.10
Seed	1.97	0.22	4.37	4.37	8.75	25	0.90:0.10
1st addition	2.34	0.26	3.02	3.02	2.25	10	0.90:0.10
2nd addition	3.78	0.42	3.80	3.80	3.50	10	0.90:0.10
3th addition	3.42	0.38	2.97	2.97	3.50	10	0.90:0.10

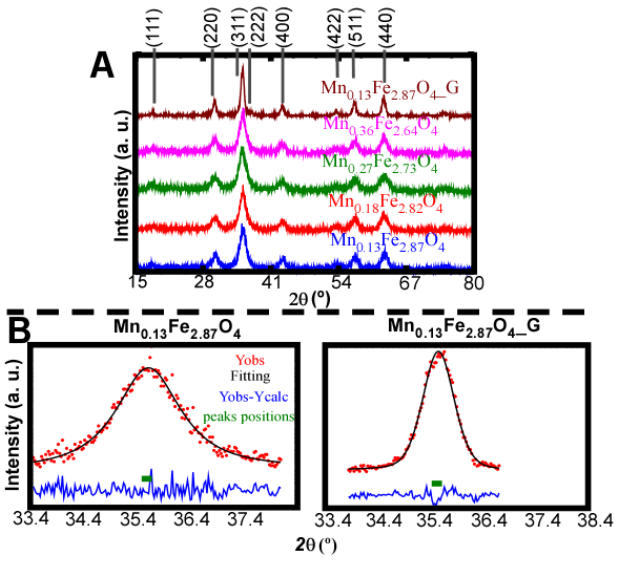

Fig. S1. (A) X Ray diffraction patterns for ferrite nanoparticles. (B) (311) peak fitting for $Mn_{0.13}Fe_{2.87}O_4$ and $Mn_{0.13}Fe_{2.87}O_4$_G samples.

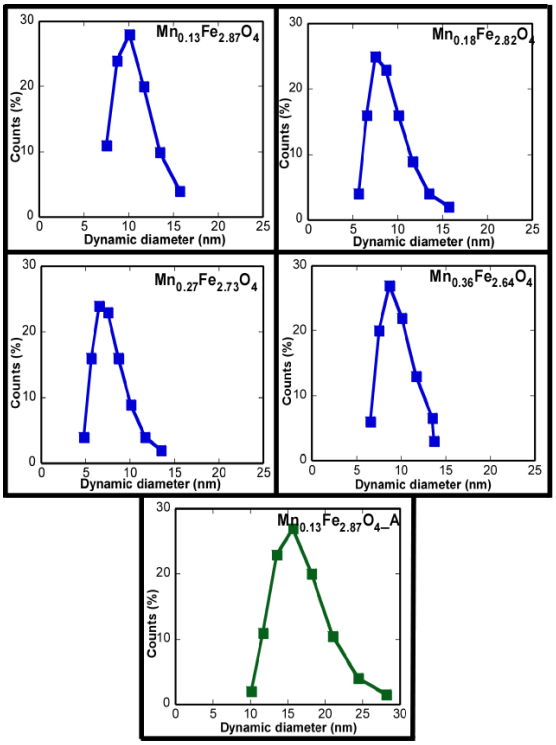

Fig. S2. Dynamic diameters of $Mn_{0.13}Fe_{2.87}O_4$, $Mn_{0.18}Fe_{2.82}O_4$, $Mn_{0.27}Fe_{2.73}O_4$, $Mn_{0.36}Fe_{2.64}O_4$ and $Mn_{0.13}Fe_{2.87}O_4$_G nanoparticle samples measured by DLS in 0.05 mgFe/mL toluene dispersions and expressed in % of total.

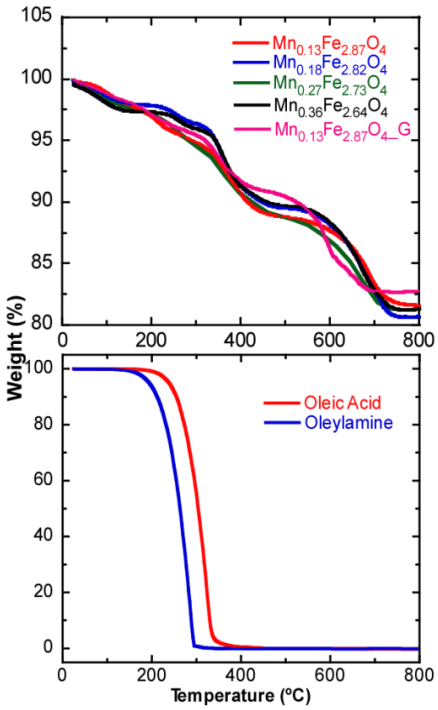

Fig. S3. Thermogravimetric curves for all prepared Mn ferrite nanoparticles measured in Ar atmosphere.

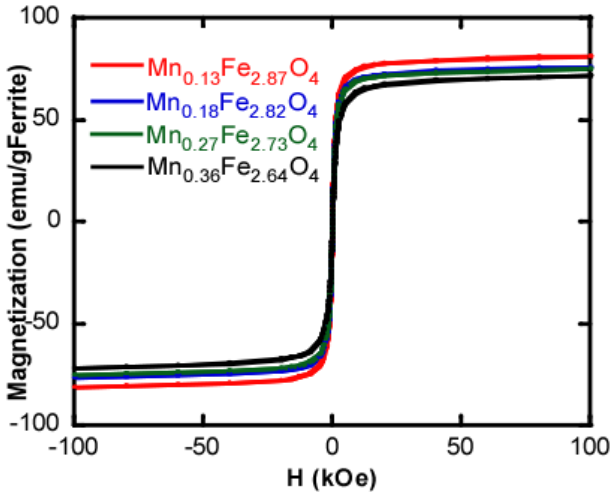

Fig. S4. M (H) cycles for all prepared Mn ferrite nanoparticles measured at 300 K in the VSM magnetometer in powder. The matrix effect in the final magnetization value has been discarded by diminishing the mass corresponding to organic matter.

Table S2. Nèel (τ_N), Brown (τ_B) and effective (τ_{eff}) relaxation times at room temperature calculated for all prepared samples. NP shape has been taken as spherical for all samples to perform this estimation. K_{eff} values at RT obtained from fitting the SAR versus H curve by LRT model (equation 5).

The Nèels relaxation time (τ_N), can be defined as an intrinsic material property and can be calculated by the following equation:

$$\tau_N = \frac{\tau_0}{2}\sqrt{\frac{\pi k_B T}{KV}}e^{KV/k_B T}$$

Where K is the materials anisotropy constant (calculated from the ZFC/FC curves), V the particle volume, T the temperature, k_B Boltzmann constant and τ_0 the attempt time, which is related to the provability of magnetic moment's spontaneous inversion in the easy magnetization axis, and is taken as 10^{-10} s for this kind of materials, as an estimation.

The Brown relaxation time (τ_B) is defined by Debye's equation, and depends on the hydrodynamic diameter of NP (r_h), fluid viscosity (η) and temperature:

$$\tau_B = \frac{4\pi\eta r_h^3}{k_B T}$$

To obtain the effective relaxation time (τ_{eff}).

$$\frac{1}{\tau_{eff}} = \frac{1}{\tau_N} + \frac{1}{\tau_B}$$

SAMPLE	T_N (s)	τ_B (s)	τ_{eff} (s)	K_{eff}(kJ/m^3)
$Mn_{0,13}Fe_{2,87}O_4$	$5.24\cdot10^{-10}$	$2.26\cdot10^{-7}$	$5.23\cdot10^{-10}$	10.4
$Mn_{0,13}Fe_{2,87}O_4$_G	$3.58\cdot10^{-8}$	$9.44\cdot10^{-7}$	$3.45\cdot10^{-8}$	(FP fit)
$Mn_{0,18}Fe_{2,82}O_4$	$2.17\cdot10^{-10}$	$1.48\cdot10^{-7}$	$2.17\cdot10^{-10}$	12.1
$Mn_{0,27}Fe_{2,73}O_4$	$2.92\cdot10^{-10}$	$1.38\cdot10^{-7}$	$2.91\cdot10^{-10}$	12.4
$Mn_{0,36}Fe_{2,64}O_4$	$2.20\cdot10^{-10}$	$1.82\cdot10^{-7}$	$2.20\cdot10^{-10}$	13.8

Model S1. Modelling single magnetic domain with thermal fluctuations. Fokker-Planck equation.

Magnetization of the single domain is represented by a vector of constant modulus (M) $\vec{M} = M\hat{r}$. The evolution of unit vector $\hat{r}$ with time is given by the dimensionless implicit Gilbert equation:

$$\frac{d\hat{r}}{dt} = \gamma\hat{r} \times \vec{B}_{eff} - \alpha\hat{r} \times \frac{d\hat{r}}{dt} \qquad \text{(S1)}$$

In this equation α is the so-called Gilbert damping constant (dimensionless constant), γ is the gyromagnetic ratio (taken as a positive number) and $\vec{B}_{eff} = (-1/M)\,\partial V/\partial\hat{r}$ ($\partial/\partial\hat{r} \equiv grad$) is the effective magnetic field, which includes the any external applied field as well as any anisotropy field of magnetocrystalline, shape or dipolar origin, $V(\hat{r})$ being the total energy density of the single domain. The dependence of $\hat{r}$ with time can be obtained explicitly after multiplying both sides of equation (S1) by ($\hat{r}\times$) operator and performing simple algebraic manipulations as:

$$\frac{d\hat{r}}{dt} = \frac{\gamma}{1+\alpha^2}\left(\hat{r} \times \vec{B}_{eff}\right) + \frac{\gamma\alpha}{1+\alpha^2}\left[\left(\hat{r} \times \vec{B}_{eff}\right) \times \hat{r}\right] \qquad \text{(S2)}$$

This is the explicit version of the dynamical equation that in the limit $\alpha \to 0$, becomes the earlier Laudau-Lifschizt equation. In (S2) the first term is responsible of the gyroscopic movement (rotation around $\vec{B}_{eff}$) and the second one accounts for the gradual reorientation of $\vec{M}$ along $\vec{B}_{eff}$. Given that $\vec{B}_{eff} = (-1/M)\,\partial V/\partial\hat{r}$, equation (S2) can be expressed as a function of energy density gradient as:

$$\frac{d\hat{r}}{dt} = -g'\left(\hat{r} \times \frac{\partial V}{\partial\hat{r}}\right) - h'\frac{\partial V}{\partial\hat{r}} \qquad \text{(S3)}$$

This is so by considering that $\hat{r} \cdot \partial V/\partial\hat{r} = 0$. Here g' and h' are constants of movement defined as: $g' = \frac{\gamma}{M(1+\alpha^2)}$ and $h' = \frac{\gamma\alpha}{M(1+\alpha^2)}$. Considering the gyromagnetic ratio of free electron, magnetization M of magnetite and a Gilbert damping constant of 0.05,

$g' \sim 360000\ (rad \cdot m^3/s \cdot J)$ and $h' \sim 18000\ (rad \cdot m^3/s \cdot J)$. In spherical coordinates, equation (S3) takes the following form:

$$\frac{d\hat{r}}{dt} = \left(\frac{g'}{sin\theta}\frac{\partial V}{\partial \varphi} - h'\frac{\partial V}{\partial \theta}\right)\hat{\theta} - \left(g'\frac{\partial V}{\partial \theta} + \frac{h'}{sin\theta}\frac{\partial V}{\partial \varphi}\right)\hat{\varphi} \qquad (S4)$$

This is a first order partial differential equation that can be solved by Runge-Kutta type algorithms. $V(\hat{r},t)$ is the energy landscape of the problem. If thermal energy is taken into account, equation (S4) must be modified to include fluctuations of the magnetization.

Thermal fluctuations . In Stoner-Wohlfart Based Models, magnetization of the single domain is well determined by a single vector that is firmly anchored to the instantaneous energy minima. However, thermal effects should bring about certain "disorder" or "fluctuation" of the single domain magnetic dipole around equilibrium orientation. In such case, magnetization should be determined not with a single vector but with a probability distribution of orientations (or representative *state* points over the unit sphere) that will be referred as $W(\hat{r},t)$. According to F.W. Brown's approach, magnetization dynamics can be understood as a current of representative points moving around the surface of the unit sphere with number density $W(\hat{r},t)$ and current density $\vec{j}(\hat{r},t)$. These representative points cannot be created nor destroyed so W and $\vec{j}$ verify the continuity equation:

$$\partial W/\partial t = -\partial \vec{j}/\partial \hat{r} \quad (or - div\vec{j}) \qquad (S5)$$

Brown postulates a diffusion contribution to the current density of the form $-k'\,\partial W/\partial \hat{r}$ in such a way that current $\vec{j}$ is given by:

$$\vec{j} = W\frac{d\hat{r}}{dt} - k'\frac{\partial W}{\partial \hat{r}} \qquad (S6)$$

Note that $\vec{j} = W\vec{v}$ in case of negligible thermal fluctuation and in this case W represents the probabilistic orientation of a large number of particles or equals the delta function for a single particle. Simply by substituting $d\hat{r}/dt$ from equation (S4) in equation (S6) the current density in spherical coordinates results in:

$$\vec{J} = -\left[\left(h'\frac{\partial V}{\partial \theta} - \frac{g'}{sin\theta}\frac{\partial V}{\partial \varphi}\right)W + k'\frac{\partial W}{\partial \theta}\right]\hat{\theta} - \left[\left(g'\frac{\partial V}{\partial \theta} + \frac{h'}{sin\theta}\frac{\partial V}{\partial \varphi}\right)W + \frac{k'}{sin\theta}\frac{\partial W}{\partial \varphi}\right]\hat{\varphi} \quad (S7)$$

Now it is enough to calculate the divergence of this current to obtain the evolution with time of the probability density W in equation (S1):

$$\frac{\partial W}{\partial t} = g'\frac{\partial}{\partial \hat{r}}\left(W\hat{r} \times \frac{\partial V}{\partial \hat{r}}\right) + h'\frac{\partial}{\partial \hat{r}}\left(W\frac{\partial V}{\partial \hat{r}}\right) + k'\frac{\partial^2 W}{\partial \hat{r}^2} \quad (S8)$$

Using very basic vector calculus rules involving *grad*, *div* and *curl*, and realizing that $div(\hat{r} \times gradV) = 0$, equation (S8) is easily transformed in :

$$\frac{\partial W}{\partial t} = g'\hat{r}\left(\frac{\partial V}{\partial \hat{r}} \times \frac{\partial W}{\partial \hat{r}}\right) + h'\frac{\partial}{\partial \hat{r}}\left(W\frac{\partial V}{\partial \hat{r}}\right) + k'\frac{\partial^2 W}{\partial \hat{r}^2} \quad (S9)$$

This is the Fokker-Planck equation ($\partial W/\partial t = L_{FP}W$) of the problem. In spherical coordinates equation (9) takes the following form:

$$\frac{\partial W}{\partial t} = \frac{g'}{sin\theta}\left(\frac{\partial V}{\partial \theta}\frac{\partial W}{\partial \varphi} - \frac{\partial V}{\partial \varphi}\frac{\partial W}{\partial \theta}\right) + h'\left(\frac{\partial V}{\partial \theta}\frac{\partial W}{\partial \theta} + \frac{1}{sin^2\theta}\frac{\partial V}{\partial \varphi}\frac{\partial W}{\partial \varphi}\right) + k'\frac{\partial^2 W}{\partial \hat{r}^2} + h'W\frac{\partial^2 V}{\partial \hat{r}^2} \quad (S10)$$

Last term contains the Laplacian operator acting over W and V. From the point of view of numerical calculations, it is more convenient to work out directly with equations (S5) and (S6), in spherical coordinates:

$$\frac{\partial W}{\partial t} = \frac{1}{sin\theta}\frac{\partial}{\partial \theta}[(sin\theta)J_\theta] + \frac{1}{sin\theta}\frac{\partial}{\partial \varphi}[J_\varphi] \quad (S11)$$

By realizing that $\vec{J} = J_\theta\vec{\theta} + J_\varphi\vec{\varphi}$ is given in equation (S7). If one can assume that gradient of distribution W is parallel to gradient of energy ($\partial W/\partial \hat{r} \times \partial V/\partial \hat{r}$) gyroscopic contribution can be dropped out from calculation.